Photogrammetrie • Fernerkundung • Geoinformation 3/2005, S. 209–218, 9 figs.

Satellite based retrieval of cloud properties and their use in rainfall retrievals and fog detection

THOMAS NAUSS, JAN CERMAK, Marburg, ALEXANDER KOKHANOVSKY, Bremen, CHRISTOPH REUDENBACH & JÖRG BENDIX, Marburg

Keywords: remote sensing, cloud properties, rainfall retrieval, fog detection

Summary: This article presents a satellite-based technique for the retrieval of cloud properties and two follow-up products. The very computer time efficient cloud property retrieval was evaluated against corresponding products of the Japanese and US space agencies (JAXA, NASA) showing good results. In addition, two examples for the use of the derived cloud parameters are shown: a highly accurate rainfall retrieval and a fog detection and clearance model.

Zusammenfassung: *Satellitenbasierte Ableitung von Wolkenparametern und deren Verwendung in Niederschlagsretrievals und Nebel-Erkennungsverfahren*. Der Artikel stellt eine Technik zur Ableitung von Wolkeneigenschaften aus Satellitendaten sowie zwei darauf aufbauende Produkte vor. Die Ergebnisse des rechenzeit-optimierten Algorithmus zeigen gute Übereinstimmungen mit den entsprechenden Produkten der japanischen und amerikanischen Weltraumbehörden (JAXA, NASA). Beispielhaft für diverse Anwendungsmöglichkeiten wird ein auf den abgeleiteten Wolkenparametern aufbauendes Niederschlagsretrieval sowie ein Modell zur Nebelerkennung und Nebelauflösung vorgestellt.

1 Introduction

Clouds play an important role in the earth-atmosphere radiation budget. Therefore many authors have developed satellite-based techniques for cloud property retrievals (e. g. ARKING 1985, NAKAJIMA & NAKAJIMA 1995). The cloud parameters themselves are of high interest for weather and climate research but they can also be used to compute further products like rainfall and fog maps or warning systems for icing in the field of general aviation (NAUSS et al. 2004). Therefore operational processing chains have been implemented at the Laboratory for Climatology and Remote Sensing (LCRS) in order to retrieve not only cloud properties but also the mentioned higher level products (cf. NAUSS & BENDIX 2005). This paper gives a short overview of the techniques used. First, the retrieval of cloud properties – namely the cloud optical thickness and the effective droplet radius – using a semi-analytical approach is presented, followed by an overview of a rainfall retrieval for the latest Meteosat system (Meteosat-8 SEVIRI) and a fog detection scheme, both of which use the cloud parameters.

2 Retrieval of cloud properties

Daytime cloud parameter retrievals rely on the well-known characteristics of the reflection function of clouds in a non-absorbing (visible) and an absorbing (near-infrared) wavelength. This principle is illustrated in Fig. 1 for wavelengths of 0.65 µm and 1.6 µm. Continuous lines represent equal effective radii, dashed lines equal values of the

1432-8364/05/2005/0209 $ 2.50

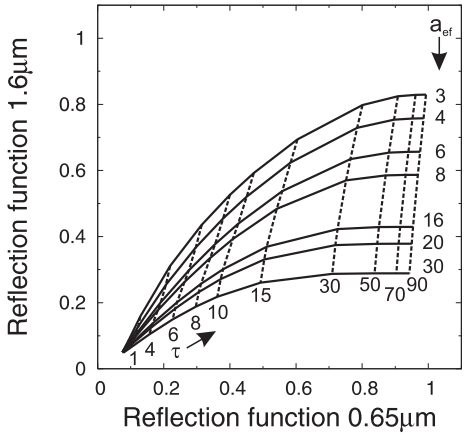

Fig. 1: Reflection function of a cloud at 0.65 µm vs. 1.6 µm as a function of optical thickness (dashed lines) and effective cloud droplet radius (solid lines) for a sun and satellite zenith angle of 0°.

optical thickness. Thus the reflection function at the non-absorbing wavelength is mainly a function of the cloud optical thickness τ and the absorbing wavelength signal is determined by the effective cloud droplet radius a_{ef} (an integrated value for the droplet size distribution function, cf. HANSEN & TRAVIS 1974).

Usually, pre-calculated reflectance values from radiative transfer simulations are iteratively lined up with actual measurements in the visible and near-infrared wavelenghts in order to retrieve τ and a_{ef} (KAWAMOTO et al. 2001, PLATNICK 2000). Because these so-called look-up table (LUT) approaches are based on exact radiative transfer computations they are very accurate when compared to theoretical reflectance functions. On the other hand, the iteration is very expensive

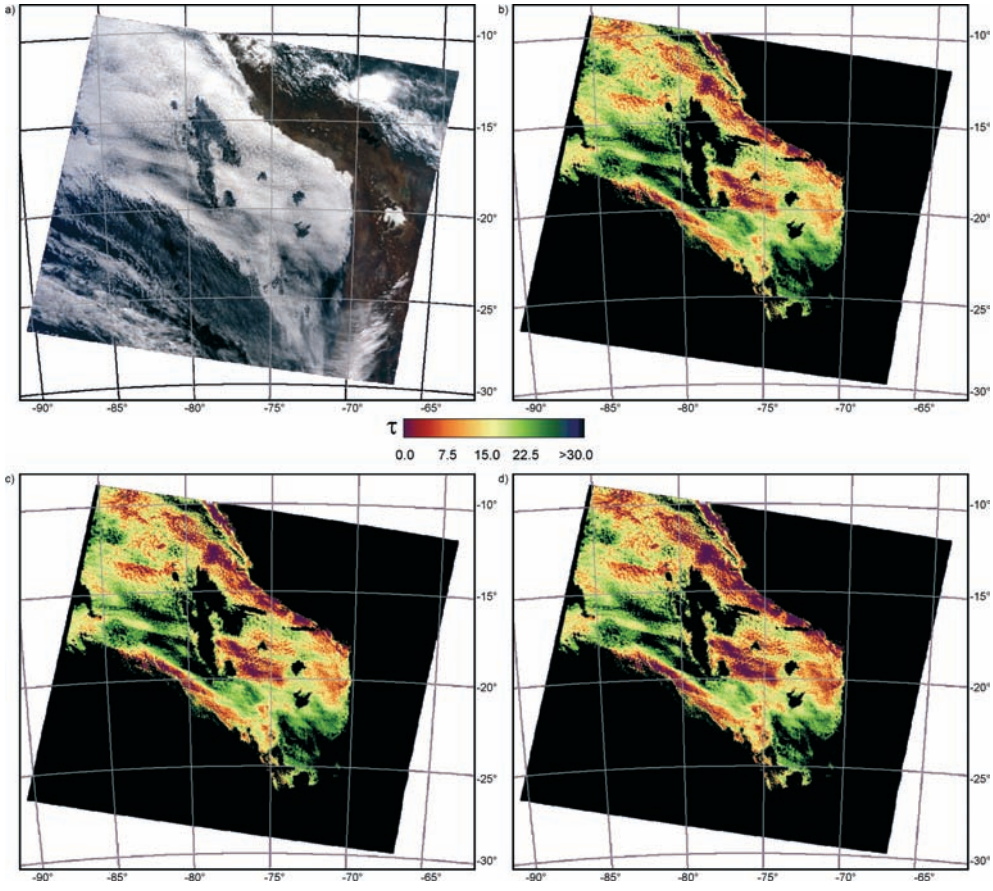

Fig. 2: Composite image (a) and optical thickness retrieved from MOD06 (b), ATSK3 (c) and SACURA (d) for Terra-MODIS scene from July 18th 2001, 15:30 UTC (NAUSS et al. 2005).

in terms of computer time. Therefore Kokhanvoksy et al. (2003) developed the semi-analytical cloud property retrieval SACURA, which is based on the approximated versions of the asymptotic radiative transfer equations (Sobolev 1984) valid for clouds with $\tau > 5$. SACURA is much more time-efficient than the LUT techniques (about factor 25), which is of great importance for operational, near real-time retrievals.

The mathematical equation of SACURA for the reflection function in a non-absorbing band is based on approximations of van de Hulst (1980) and can be expressed by the reflection function of a semi-infinite cloud, the diffuse transmittance and the escape function. Therefore the calculation of the reflection function of a finite cloud is reduced to that of a semi-infinite one, which only depends on the phase function, and even this dependence is rather weak. The reflection function of a semi-infinite cloud is calculated for a one-degree grid using the exact radiative transfer code of Mishchenko et al. (1999) for a modified gamma distribution and effective radius of 6 µm whereby the influence of a_{ef} is negligible (Kokhanovsky 2004a).

Besides its dependence on τ, the diffuse transmittance itself is a function of the asymmetry parameter and the escape function, which can be approximated with high

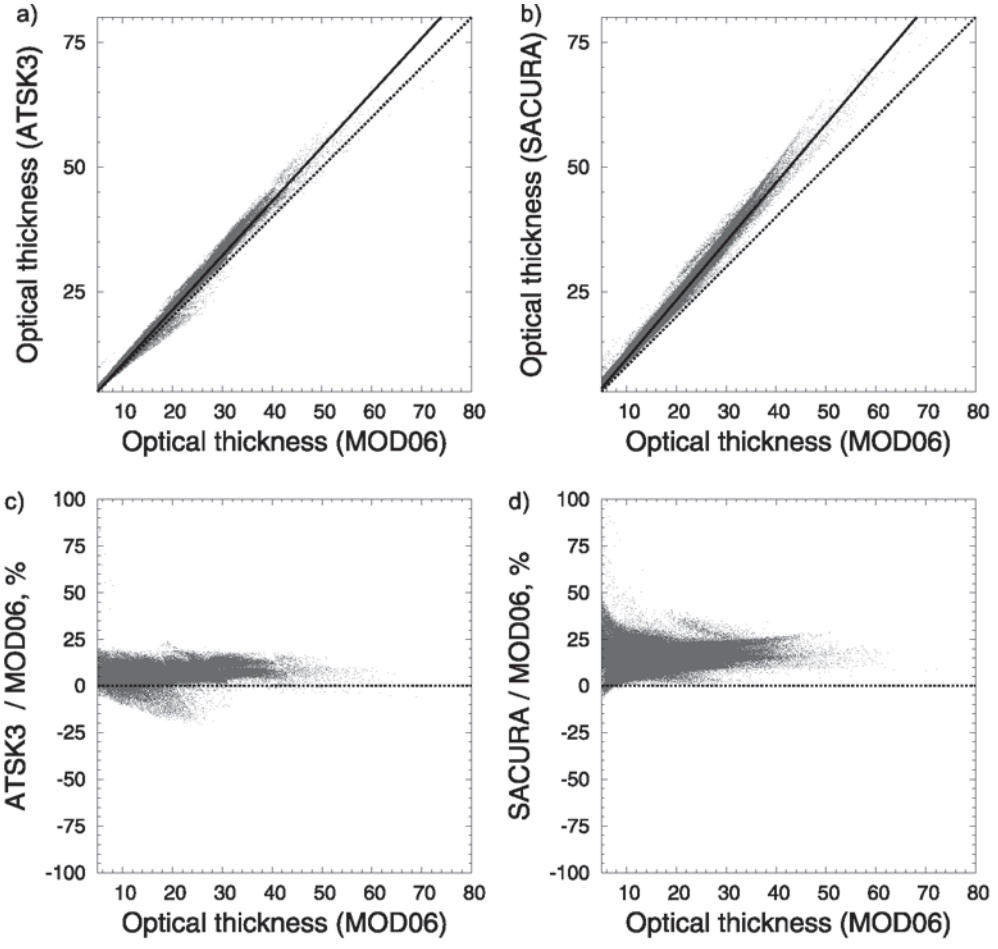

Fig. 3: Optical thickness retrieved by ATSK3 (a) and SACURA (b) vs. MOD06 and corresponding percentage difference (c, d) for Terra-MODIS scene from Fig. 2 (Nauss et al. 2005).

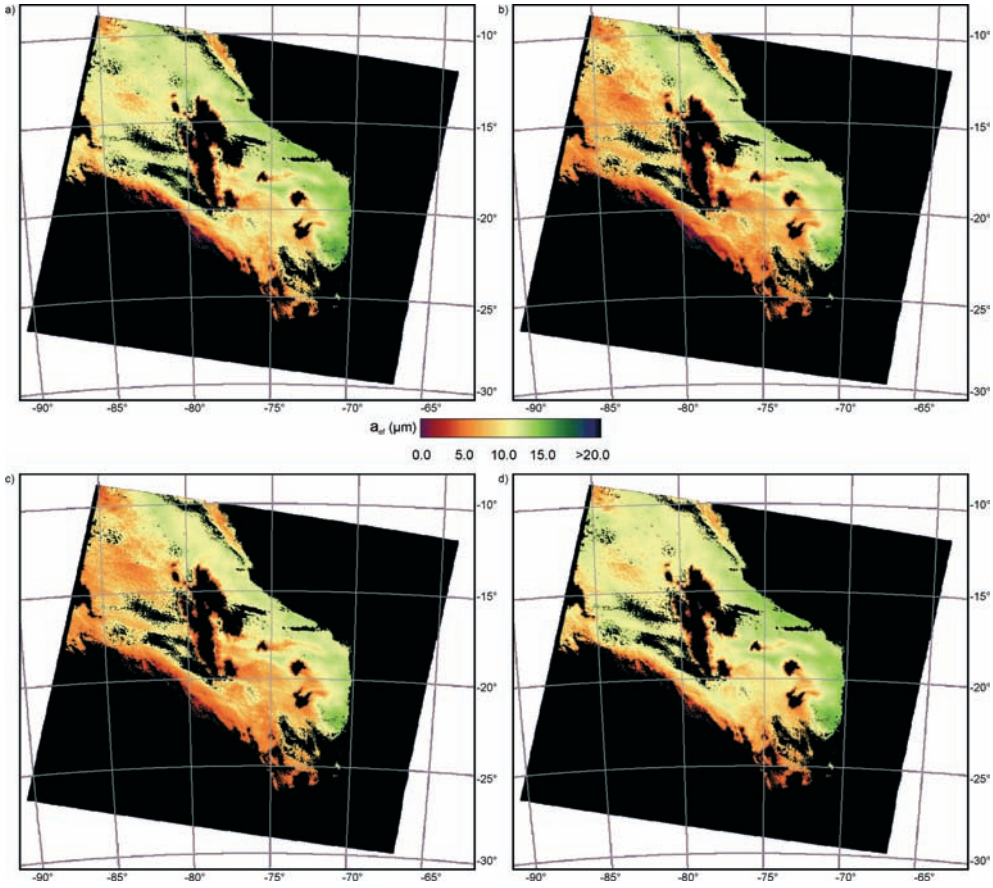

Fig. 4: Composite image (a) and effective cloud droplet radius retrieved from MOD06-37 (a), MOD06-16 (b), ATSK3 (c) and SACURA (d) for Terra-MODIS scene from Fig. 2 (NAUSS et al. 2005).

accuracy (KOKHANOVSKY 2004b). The latter takes into account the probability that under a given viewing geometry a photon is scattered in the direction of the sensor.

In the near infrared range the reflection function of an absorbing cloud can be found from the solution of integral equations (NAKAJIMA & KING, 1992). For SACURA, several exponential solutions (ZEGE et al. 1991, KOKHANOVSKY et al. 2003) are used, which are valid if the probability of photon absorption is small. This is usually the case for water clouds in the visible and near-infrared spectrum (KOKHANOVSKY 2004a).

Since the reflection function of a cloud in the visible band is not only a function of τ but also of a_{ef}, which enters the equations by its influence on the asymmetry parameter, the optical thickness cannot be retrieved by measurements in the non-absorbing band alone. On the other hand, the reflection function in the near-infrared band depends on the liquid water path, which itself can be expressed as a function of τ, a_{ef} and the diffuse transmission (the latter taken from the reflection function in the visible channel). The substitution of the liquid water path by these parameters yields a single equation for the retrieval of the cloud properties and can easily be solved numerically. For details on SACURA, cf. KOKHANOVSKY et al. (2003).

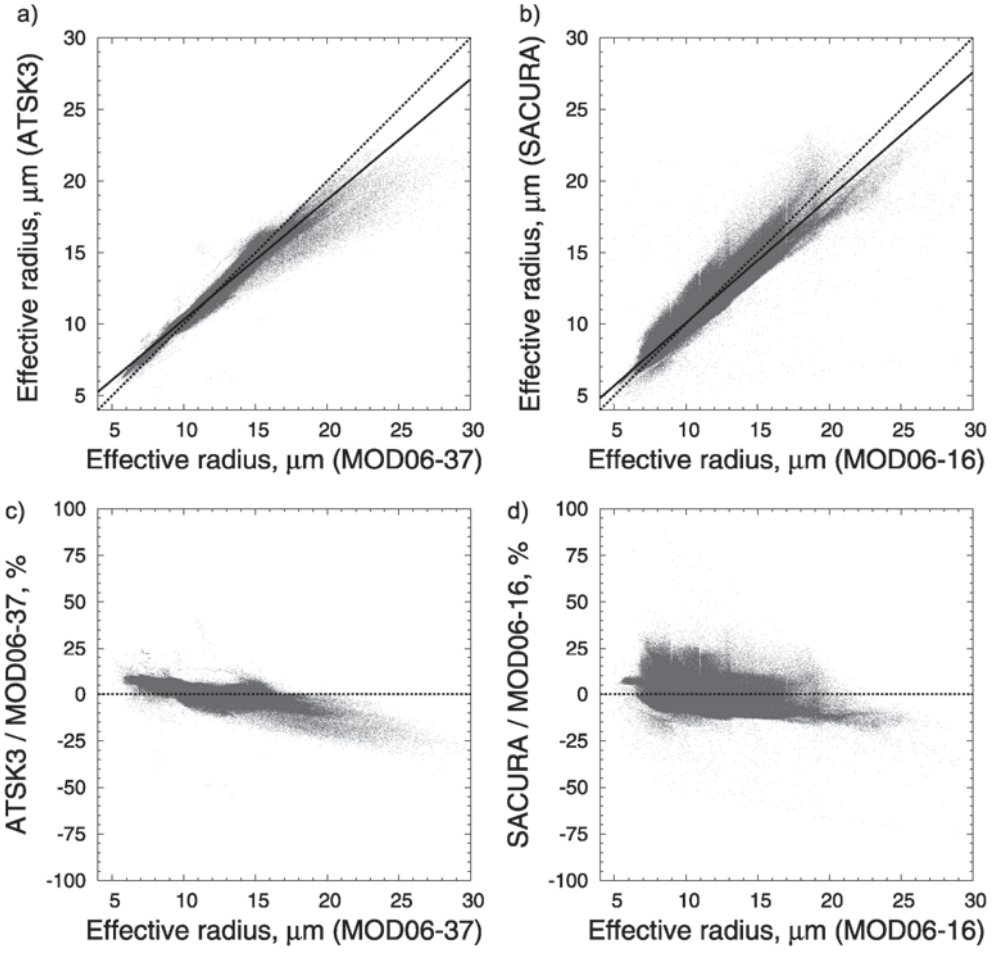

Fig. 5: Effective cloud droplet radius retrieved by ATSK3 (a) and SACURA (b) vs. MOD06-37 and MOD06-16 respectively and corresponding percentage difference (c, d) for Terra-MODIS scene from Fig. 2 (NAUSS et al. 2005).

SACURA has been evaluated against the ATSK-3 retrieval by the Japan Aerospace Exploration Agency (JAXA, KAWAMOTO et al. 2001) and the MODIS cloud property product MOD06 (PLATNICK et al. 2003) of the US National Aeronautics and Space Administration (NASA). All three retrievals show good correlations over oceans as well as over land with a squared correlation coefficient (r^2) larger then 0.94 for τ and larger then 0.79 for a_{ef} (see KOKHANVOSKY et al. 2005, NAUSS et al. 2005). An example is shown in Fig. 2 for a scene of the Terra-MODIS polar orbiting system on 18 July 2001, 15:30 UTC over the eastern Pacific and the western part of south America. As can be seen in Fig. 3 the correlation between the optical thickness retrieved by MOD06, ATSK-3 and SACURA respectively fit very well, with an r^2 of 0.99 in all cases. Both, ATSK-3 and SACURA tend to retrieve larger values of τ as compared to MOD06. Fig. 4 shows the retrieved effective radius. Since ATSK-3 uses near-infrared data at 3.7 µm while SACURA uses the 1.6 µm channel, the retrievals are compared to different versions of the MOD06 product using the appropriate channels in each case

(MOD06-16 and MOD06-37). The corresponding plots are shown in Fig. 5. Again, there is a quite good correlation with an r^2 of 0.99 (ATSK-3) and 0.94 (SACURA) respectively.

3 Rainfall Retrieval based on cloud properties

The straightforward approaches of satellite-based rainfall retrievals normally identify convective precipitating clouds by means of their infrared brightness temperature. This usually works well in the tropics but cannot simply be applied to the complex situation of mid-latitude frontal precipitation. Hence, a new technique has been developed for Meteosat-8 SEVIRI, which is also applicable to advective/stratiform precipitation in the mid-latitudes. It consists of two modules. The first deals with precipitation from convective core areas, the second with that of advective/stratiform precipitating clouds.

The convective module is based on the Enhanced Convective Stratiform Technique (ECST, Reudenbach 2003) that uses positive temperature differences between the water vapour and infrared channels (d_{WI}) in order to discriminate between deep convective, optically thick clouds ($d_{WI} > 0$) and non-raining cirrus ($d_{WI} < 0$, cf. Tjemkes et al. 1997). Pixels with positive d_{WI} are then subdivided by analysing the frequency distribution of the infrared brightness temperatures (TB_{IR}). Areas with $TB_{IR} < 1^{st}$ quartile of the frequency distribution represent overshooting tops of convective cores, those in the 1st quartile reveal raining systems at tropopause level and pixels with $TB_{IR} < 3^{rd}$ quartile identify potentially raining cloud systems of great vertical extension. As a result, isolated convective cores can be distinguished from directly adjacent stratiform raining areas.

The advective/stratiform module is based on the concept that potentially raining cloud

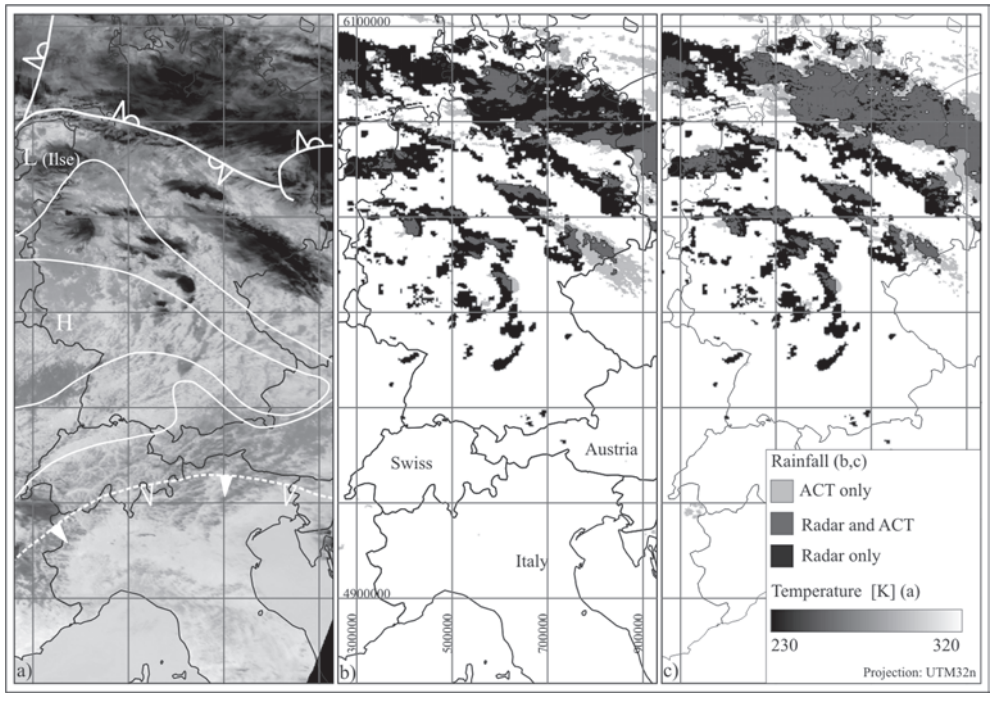

Fig. 6: Terra-MODIS data during the Elbe flood for August 5th 2002, 11:05 UTC, showing (a) infrared data overlayed by the synoptic situation, (b) the results of the ACT convective module merged with data from the C-band radar network of the German weather service and (c) the same merge but with the additionally activated ACT cloud property module.

systems require both a certain size of droplets that can fall out of the cloud against the updraft wind field and a minimum cloud thickness that allows droplets to grow large enough and prevents them from evaporating below the cloud base (see also LENSKY et al. 2003). Therefore, 225 satellite scenes have been analysed together with data from the ground based radar network of the German weather service (DWD) to find a discrimination function that delineates raining from non-raining areas, using a variable threshold value of a_{ef} as a function of τ. The potential benefit of this identification scheme is shown in Fig. 6 for a scene during the severe flood events on August 5th 2002, 11:05 UTC. It shows the complex situation with low pressure system *Hanne* centred over the north-western Netherlands causing extensive stratiform cloud areas along the occlusion in the north/north-eastern part of the scene and shallow convection over the alps indicating a dissolving cold front. Between these frontal regions intensive convection due to a high pressure ridge extending from France to central Germany can be clearly identified in the Terra-MODIS infrared image (Fig. 6a). Fig. 6b presents an overlay of radar network data (C-band) of the German Weather Service and the retrieval results using only the convective module of the rainfall retrieval. Both, the shallow convection along the cold front over the Alps/south-western Germany and the convective systems over France and the German mountain foreland are identified correctly as non-raining and rainfall is assigned to the cloud clusters along the border of the high pressure ridge. Nevertheless, only areas close to the tropopause in the northern stratiform band where identified as raining. In Fig. 6c. the advective/stratiform scheme was additionally used for the retrieval. The identified raining area now covers almost the entire northern cloud band and the isolated systems in the centre are also well detected.

4 Fog detection based on cloud properties

Microphysical parameters play a crucial role in the operational fog detection and dissipation schemes used at the LCRS. In the former, cloud optical depth and droplet effective radius are used in a plausibility test. The latter scheme makes use of liquid water path and of cloud geometrical thickness derived from cloud optical depth.

The fog detection technique consists of a series of individual tests comprising both, pixel-based and object-oriented components. A summary of the entire scheme is given in Fig. 7 and described in detail in CERMAK & BENDIX (forthcoming). As can be seen here, fog is treated as a residual category after the explicit exclusion of other classes. In a first step, all non-cloud pixels

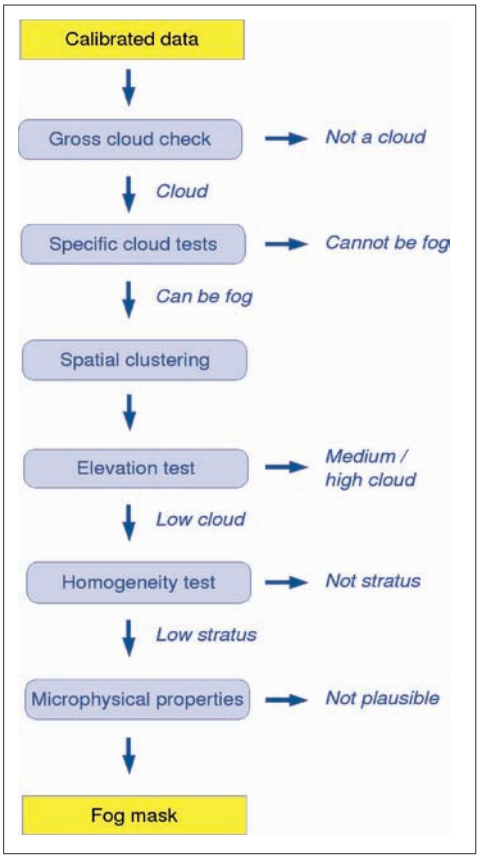

Fig. 7: Overview of the fog detection scheme.

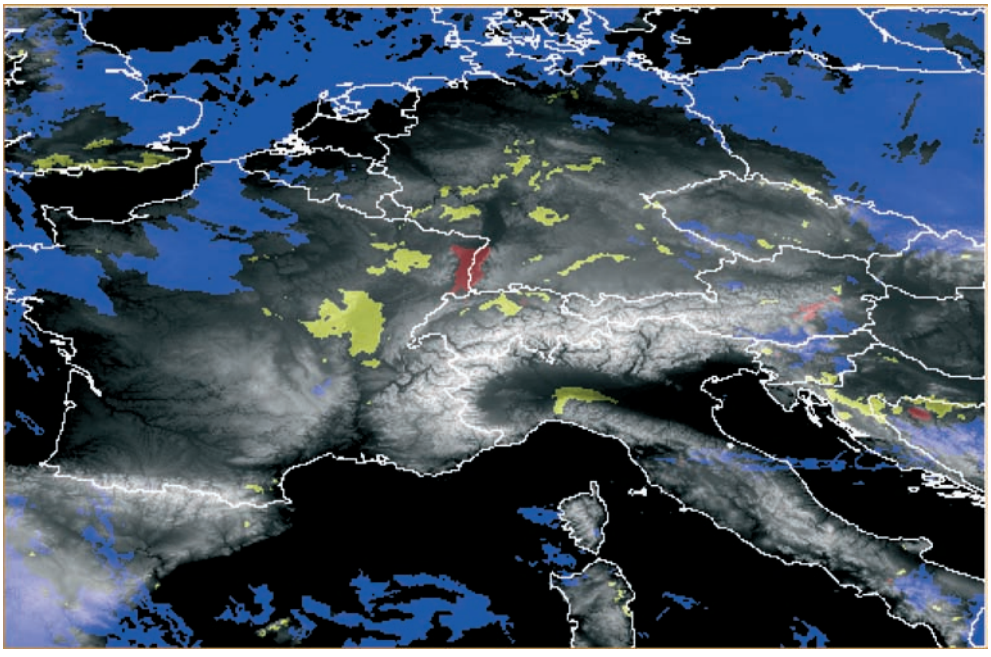

Fig. 8: Meteosat-8 SEVIRI fog map for November 5th 2003, 09:00 UTC. Yellow and red areas are fog, blue areas other water clouds.

are rejected by means of a gross cloud check. This test makes use of the radiances received at the sensor at 10.8 and 3.9 µm. Due to the solar signal in the latter channel the radiance difference of the two channels ($R_{10.8} - R_{3.9}$) is smaller for cloud-contaminated than for clear pixels. Any pixels identified as cloud-covered then undergo tests to exclude a number of non-fog clouds and snow. These tests are based on a number of spectral channels. After this step all remaining cloud areas potentially qualify as fog. These regions are then clustered into spatially discrete and coherent entities for further testing. Each entity is assessed in terms of elevation and surface homogeneity. Where either criterion is outside a predefined range the cloud entity is flagged as non-fog.

Finally, a microphysics-based plausibility test eliminates any pixels with droplet radii or cloud optical depths beyond the range observed in fog. Standard values for both parameters were retrieved from the literature (e. g. Tampieri & Tomasi 1976, Pinnick et al. 1978). According to these sources, fog optical depth normally ranges between 0.15 and 30 while droplet effective radius varies between 3 and 12 µm, with a maximum of 20 µm in coastal fog. These values are tested against those retrieved operationally in the scheme presented above. The microphysics component is of particular importance in the scheme because it helps ensure the physical plausibility of the fog mask product. A sample of the finished fog mask product for November 5th 2003, 09:00 UTC, can be seen in Fig. 8.

Once a fog mask has been derived, a thermo-dynamical model is run to compute the fog dissipation time for each fog-covered pixel. This scheme again makes use of microphysical parameters: As input the fog dissipation model uses the 0.6 and 10.8 µm channels, the fog mask product, radiosounding data, a digital elevation model, cloud optical thickness, droplet effective radius, liquid water path and cloud geometrical thickness.

The assumption of the model is that fog clearance happens where the temperature at time t (T_t) reaches a required fog clearance temperature (T_c):

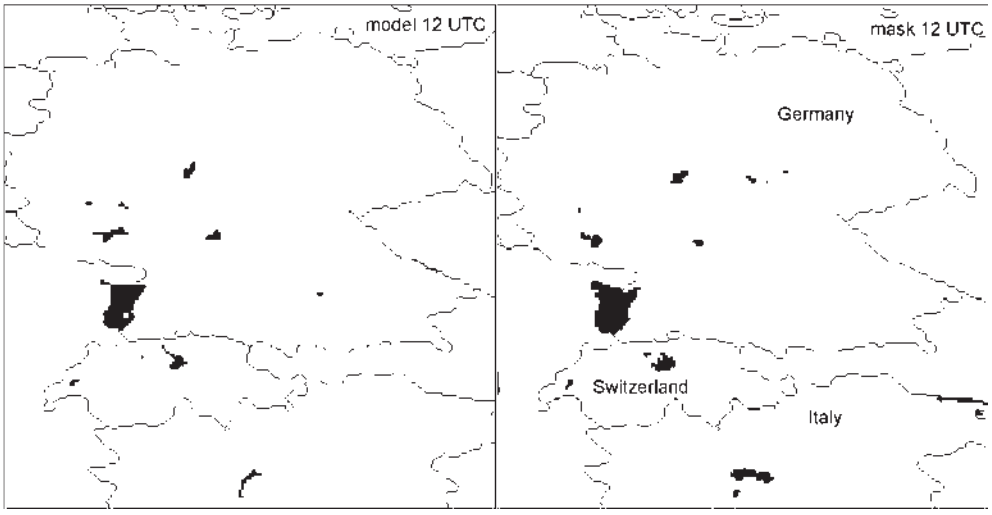

Fig. 9: Fog clearance model result for November 5th 2003, 12 UTC based on the fog map of Fig. 7 (left) and actual fog map for 12:00 UTC (right).

$$T_t(d_z, R_{0.6}, R_{10.8}, \Theta) = T_c(d_z, LWP, r_w, \Gamma) \quad (1)$$

T_t is computed as a function of cloud geometrical thickness (d_z), the radiances at 0.6 ($R_{0.6}$) and 10.8 µm ($R_{10.8}$), and the solar zenith angle (Θ). Geometrical thickness is computed using an empirical parameterization based on cloud optical depth. T_c (fog clearance time) is defined as the time when all fog droplets within a pixel evaporate. It depends on cloud thickness, liquid water path, saturation humidity mixing ratio (r_w), and the atmospheric temperature lapse rate (Γ). The cloud liquid water path is computed from droplet effective radius and cloud optical depth using the relationship shown in equation (8).

A more detailed description of the fog dissipation model can be found in Reudenbach & Bendix (1998). The operational availability of microphysical information computed in the above scheme allows for this model to run continuously. A sample model result can be seen in Fig. 9. This mask is based on a fog mask product of November 5th 2003, 9:00 UTC. The left hand side of the figure shows the model output for 12 UTC, the corresponding mask can be seen on the right. Both images show good agreement of fog areas indicating.

Acknowledgements

This work was supported by the German Federal Ministry for Education and Research (BMBF) in the scope of the GLOWA-Danube project 07 GWK 04 "Rainfall Retrieval" and by the DFG (projects BU 688/8-1 and 1780/8-3).

References

Arking, A. & Childs, J.D., 1985: Retrieval of cloud cover parameters from multispectral satellite images. – Journal of Applied Meteorology **24:** 322–333.

Cermak, J. & Bendix, J., (forthcoming): A Daytime Scheme for the Automated Detection of Fog and Low Stratus Using MSG SEVIRI Data. – Submitted to Journal of Geophysical Research.

Hansen, J.E. & Travis, L.D., 1974: Light scattering in planetary atmospheres. – Space Science Reviews **16:** 527–610.

Kawamoto, K., Nakajima, T. & Nakajima, T.Y., 2: A Global Determination of Cloud Microphysics with AVHRR Remote Sensing. – J. Climate **14:** 2054–2068.

Kokhanovsky, A.A., 2004a: Reflection of light from non absorbing semi-infinite cloudy media: a simple approximation. – Journal of quantitative Spectroscopy and radiative Transfer **85:** 25–33.

Kokhanovsky, A.A., 2004b: Light Scattering Media Optics. – rd ed., Springer Verlag, Berlin.

Kokhanovsky, A.A., Rozanov, V.V. Zege, E.P., Bovensmann, H. & Burrows, J.P., 2003: A semi analytical cloud retrieval algorithm using backscattered radiation in 0.4–2.4 µm spectral region. – Journal of Geophysical Research **108:** 4-1–4-19.

Kokhanovsky, A.A., Rozanov, V.V., Nauss, T., Reudenbach, C., Daniel, J.S., Miller, H.L. & Burrows, J.P., 2005: The semi analytical cloud retrieval algorithm for SCIAMACHY. I. The validation. – Atmospheric Chemistry and Physics; accepted for publication.

Lensky, I.M. & Rosenfeld, D., 2003: Satellite-based insights into precipitation formation processes in continental and maritime convective clouds at nighttime. – Journal of Applied Meteorology **42:** 1227–1233.

Mishchenko, M.I., Dlugach, J.M., Yanovitskij, E.G. & Zakharova, N.T., 1999: Bidirectional reflectance of flat, optically thick particulate layers: An efficient radiative transfer solution and applications to snow and soil surfaces. – Journal of Quantitative Spectroscopy and Radiative Transfer **63:** 409–432.

Nakajima, T. & King, M.D., 1992: Asymptotic theory for optically thick layers: Application to the discrete ordinates method. – Applied Optics **31:** 7669–7683.

Nakajima, T.Y. & Nakajima, T., 1995: Wide-area determination of cloud microphysical properties from NOAA AVHRR measurements for FIRE and ASTEX regions. – J. Atmos. Sci. **52:** 4043–4059.

Nauss, T. & Bendix, J., 2005: An operational MODIS processing scheme (MOPS) for PC. – Computers and Geoscience, accepted for publication.

Nauss, T., Kokhanovsky, A.A., Nakajima, T.Y., Reudenbach, C. & Bendix, J., 2005: The intercomparison of selected cloud retrieval algorithms. – Atmos. Res., accepted for publication.

Nauss, T., Reudenbach, C., Cermak, J. & Bendix, J., 2004: Operational identification and visualisation of cloud processes for general aviation using multispectral data. – Proceedings of the 2004 Eumetsat Meteorological Satellite Conference.

Pinnick, R.G., Hoihjelle, D.L., Fernandez, G., Stenmark, R.B., Lindberg, J.D., Hoidale, N.T. & Jenninges, S.G., : Vertical structure in atmospheric fog and haze and its effect on visibility and infrared extinction. – Journal of Atmospheric Sciences **35:** 2020–2032.

Platnick,S., 2000: Vertical photon transport in cloud remote sensing problems. – Journal of Geophysical Research **105:** 22919–22935.

Platnick, S., King, M.D., Ackerman, S.A., Menzel, W.P., Baum, B.A., Riédi, J.C. &. Frey, R.A., 2003: The MODIS cloud products: Algorithms and examples from Terra. – IEEE Transactions on Geoscience and Remote Sensing **41:** 459–473.

Reudenbach,C., 2003: Convective summer precipitation in Central Europe. – Bonner Geogr. Abh. **109**, 152 pp., Sankt Augustin. [German]

Reudenbach, C. & Bendix, J. : Experiments with a straightforward model for the spatial forecast of fog/low stratus clearance based on multisource data. – Meteorological Applications **5:** 205–216.

Sobolev, V.V., 1984: Integral relations and asymptotic expressions in the theory of radiative transfer. – Astrofizika **20:** 123–132.

Tampieri, F. & Tomasi, C., 1976: Size distribution of fog and cloud droplets in terms of the modified gamma function. – Tellus **28:** 333–347.

Tjemkes, S.A., van de Berg, L. & Schmetz, J.: Warm water vapour pixels over high clouds as observed by Meteosat. – Beiträge zur Physik der Atmosphäre **70:** 15–21.

Van de Hulst, H.C., 1980: Multiple light scattering: Tables, formulas and applications. – Academic Press, New York.

Anschriften der Autoren:

Dipl.-Geogr. Thomas Nauss, Jan Cermak MA, Dr. Christoph Reudenbach & Prof. Dr. Jörg Bendix, Marburg
Laboratory for Climatology and Remote Sensing, University of Marburg
Deutschhausstr. 10, D-35032 Marburg
e-mail: nauss@lcrs.de

Dr. Alexander Kokhanovsky, Bremen,
Institute of environmental Physics, Bremen University, Otto-Hahn-Allee 1, D-28334 Bremen

Manuskript eingereicht: Januar 2005
Angenommen: Februar 2005